JOURNAL OF OPTOELECTRONICS AND ADVANCED MATERIALS Vol. 10, No. 11, November 2008, p. 3117 - 3123

Review Paper

A way to increase the critical current in high temperature superconductors: neutron irradiation

V. SANDU
National Institute of Materials Physics, 105 b Atomistilor Str., Magurele, 077125 Romania

Neutron irradiation is a promising method for a spectacular enhancement of the critical current density of the high temperature superconductors. The suppression of the mechanisms responsible for superconductivity under irradiation are analyzed and put side by side with the effects on the flux line lattice dynamics. Additionally, the evolution of the creation/generation balance of the defects of the crystal structure is connected to the evolution of the response of the vortex system with an emphasis on the ceramic materials.

(Received October 20, 2008; accepted October 30, 2008)

Keywords: Critical current, Superconductor, Neutron irradiation

1. Introduction

The large scale use of the superconducting materials in current transport, high magnetic field generation, and energy storage requires the capability to transport high current density without dissipation. This is possible only in type 2 superconductors that posses a critical field high enough to allow superconductivity in a large field range. The magnetic field is not perfectly screened in this class of superconductors, but the field penetrates the materials as flux tubes carrying a flux quantum $\Phi_0 = \frac{h}{2e}$ rounded by screening currents that prevent the diffusion of the field inside the rest of the sample. This complex object: flux line dressed with screening currents, known as vortex, can be moved through the sample by a driving current J due to the Lorentz force $F_L = J\Phi_0$. The motion of a flux tube, however, generates an electric field, hence, a nonzero Poynting vector. Therefore, if vortices are not immobilized in a certain way any transport current, no matter how small it is, would generate dissipation. Fortunately, vortices can be pinned in those sites where superconductivity is suppressed at scales of order of the Ginzburg-Landau coherence length ξ (the distance of the decay of the superconducting order parameter). These sites behave like potential wells for vortices, hence, are characterized by a *pinning force* that can be overwhelmed only for current density higher than a threshold value J_c.

The case of high temperature superconductors (HTS) is a special one. They are extremely attractive due to the high critical temperature alowing them to operate with cheap cryogenic liquids but have the drawback of a weak pinning as well as the bad mechanical properties. Therefore, the first challenge is the artificial creation of pinning centers and an increase of their pinning strength. However, this is not a trivial task because these class of materials have a very small coherence length ξ, of the order of the elementary crystalline cell, that makes difficult the creation and uniform disemination of such small normalized areas within a superconducting material. The tools available for such a process are either chemical insertion of pinning centers or defect creation by irradiation. Obviously, the first way is cleaner but less effective in spreading inclusions of nanometric size in a material very sensitive to stoichiometry. Additionally, the point defects are uncorrelated and act statiscally on the vortex line [1].

The use of nuclear particle is more effective because the extremelly high energy deposited in these materials is able to create more correlated deffects with a much stronger pinning force. By far, the strongest pinning was produced with very energetic (of order GeV) heavy (Z > 50) ions [2,3]. The energy deposited during irradiation creates columnar deffects tracking the ion paths which catch the vortices almost on the entire length. This method is limited to thin films and thin single crystals due to the small stopping path of the charged particles.

This thickness limitation is overcome by the use of neutrons which have the advantage of the electrical neutrality, hence, of a long mean free path in the matter $l \approx 1 \div$ d 10 cm. The physics of the interaction with the consed matter is strongly dependent on the neutron energy. High energy neutrons, E > 0.1 MeV, act by dirrect knock on with ionic species that are dislocated, thus creating Frenkel defects, and aquire high enough energy to produce in turn new dislocation up to the final stopping in a crystal sink. At low energies, E < 0.1 MeV, the interaction takes preponderantly place by neutron capture and destabilization of the target ion which breaks down in fission fragments of extremely high kinetic energy. The fragments interact with the ions of the lattice expelling them from their stable location as in the previous case.

While the use of high energetic particle is extremely expensive, the use of the neutron is hindered by the negligible effective cross section σ of neutron interaction

with the constituents of most oxide superconductors of applicative interest (σ of order unity). Therefore, large fluences, of order 10^{19} neutrons/cm^2 would be necessary to obtain sensible effects but the cost paid is the suppression of superconductivity. Fortunately, there is the option of the use of dopants with high effective cross section. The only requirement for these dopants is to be non poisonous for superconductivity. Such a friendly dopant could be lithium whose isotope ^{6}Li has a large cross section for neutron capture $\sigma(^6\text{Li})$ = 946 barn and realease very energetic alpha particles in agreement with the reaction:

$$^1\text{n}+^6\text{Li} \rightarrow {}^3\text{H}(2.77\ \text{MeV}) + {}^4\alpha(0{,}05\ \text{MeV})$$

Additionally, Li was found to enhance superconductivity whether a proper way to insert is chosen [4-7]. Our attempts to use boron, that has the highest cross section, $\sigma(^{10}\text{B})$ = 4090 barn, were not successful.

The main limitation of the pinning enhancement by neutron irradiation is the sample activation. For the superconductors belonging to the $YBa_2Cu_3O_{7-\delta}$ class (Y-123), this effect is however reduced, so that at a fluence of 7.36×10^{18} neutroni/cm^2 the effective dose is only 0.05 mSv/year g [8]. Important problems arise when materials like Ho-123, Yb-123, and Sm-123 are used because they produce a ten times higher activity or when the level of impurities is imperfectly controlled.

Although the insertion of Li proved to be the right way to improve the capture of neutrons, it is to notice that only the isotope ^{6}Li showing the largest cross section has a natural abundance which is limited to 7% in the natural Li. Therefore, the use of fluences of order $10^{17} \div 10^{17}$ remains necessary. The irradiation with such high fluences in a reasonable experimental time requires neutron flux densities as high as 10^{13} neutrons/cm^2 sec. The cheapest way to reach such high values of flux density is to perform the irradiation in the hot chamber of the reactor where the percentage of thermal and epithermal neutrons is around 80%. Additionally, the local temperature is acceptable, around 40°C, hence, there is no risk of the loss of chain oxygen of multiple layered superconductors.

Next, we focus on the on the effects of neutron irradiation performed on Li-doped Y-123 ceramics. Most results reported here have been obtained in the last decade by the Superconducting group from NIMP. The paper is structured as follows; first we present the manner of insertion of lithium. In the second section are presented the morphostructural effects of irradiation with neutrons. Section III is dedicated to the normal-superconducting transition and transport phenomena. Finally, in Section IV, the effect of neutron irradiation on the magnetic properties, including the critical current density, is presented.

2. Lithium insertion

The ceramic samples were prepared by solid state reaction from high purity reagents: Y_2O_3, CuO, and $BaCO_3$. Lithium was added in small amount to the stoichiometric mixture of the previous oxides using different Li-compounds. The preparation is well known and involves calcinations and sintering processes in flowing oxygen for 24 hours at temperatures in the range 940-960 °C. As lithium vectors were used LiF, LiCl, Li_2CuO_2, LiOH, Li_2O, Li_2CO_3, $Li_2B_4O_7$, and Li_3PO_4.

The best results were obtained with the first three compounds whereas the insertion of $Li_2B_4O_7$ depresses the superconductivity and the last compound suppresses it. X-ray diffraction showed a slow decrease of the orthorhombicity with increasing Li amount. A remarkable orthorhombic split, ε = 0.0183, was found for the samples with 2% at Li inserted via LiF which is higher than in optimally doped Y-123 (ε = 0.0174).

SEM studies show that in the best samples (with Li-halides) the crystallites are polyhedral in shape with a large dimensional dispersion (10-100 μm) (see Fig. 1 a). It is interesting that the use of LiOH produces very large grains (Fig. 1 b).

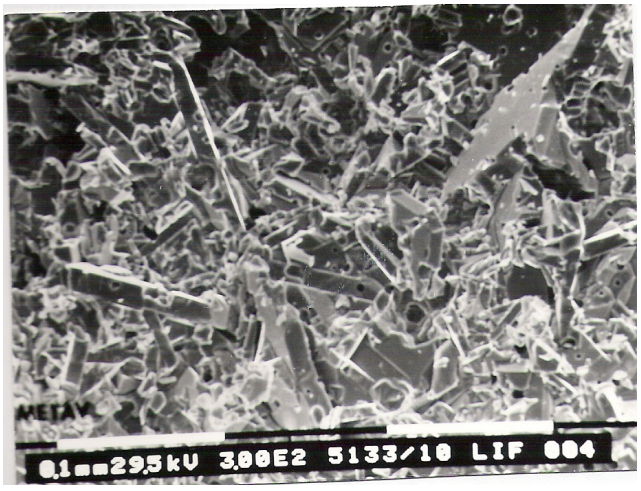

a

b

Fig. 1. Micrographies of a Y-123ceramic sample doped with Li via LiF (a) and LiOH (b)

The main results regarding the doping with lithium are summarized in the Table 1.

Table 1. Critical temperature T_c and orthorhombic split ε for Li-doped $YBa_2Cu_3O_7$ samples.

	$YBa_2Cu_3O_{7-x}(LiF)_y$				$YBa_2Cu_3O_{7-x}(LiCl)_y$			$YBa_2Cu_3O_{7-x}(Li_2CuO_2)_y$		
Y	0.02	0.06	0.10	0.12	0.02	0.04	0.06	0.02	0.04	0.06
ε	0.0183	0.0174	0.0171	0.0162	0.0171	0.0171	0.0173	0.0170	0.0168	0.0153
T_c(K)	93.48	91.92	92.38	88.84	91.30	93.50	92.19	91.46	89.74	88.8

3. Microstructural effects of neutron irradiation

Transmission electron microscopy (TEM) investigation has shown that neutron fluences, $\Phi < 10^{17}$ neutrons/cm^2, increase the density of twin lamellae [9] relative to the virgin sample. At higher fluences, a twin fading and, further, twin fragmentation occurs. Typical for the latter is the presence of a tweed structure. It might be the result of an oxygen loss because similar structure were reported in underdoped Y-123 [10, 11].

The defects associated with this fluence range consist in clusters of point defects (Frenkel defects). The density of dislocation loops and stacking faults is still reduced at 1.02×10^{17} neutrons/cm^2. Dislocation loops of 100 Å s could be good effective pinning centers. The density of dislocation loops increases with the neutron fluence and finally overlap. Therefore, at the highest fluence, large areas of normalized material are currently observed. Cellular structures were also reported in Y-123 at very high fluences [12, 13]. At fluences as high as 5×10^{17} neutrons/cm^2, a massive proliferation of fine (around 200 Å) Cu_2O particles were detected. But the obvious shrinkage of the elementary cell suggests a possible insertion of Li. At even higher fluences, the density of $(Cu,Li)_2O$ particles increases fast whereas the average size drastically decreases [9].

The increase of the dislocation loops density as well as the proliferation of tiny nonsuperconducting $(Cu,Li)_2O$ particles produced at intermediate at high fluences explain the spectacular enhancement of pinning in Y-based cuprates. Obviously, there is a threshold above which the proliferation of defects leads to a general suppression of superconductivity decreasing the interest for this method as a useful tool for pinning enhancement.

4. Normal superconducting transition and transport properties.

Generally, irradiation increases the density of scattering centers; hence, it is supposed to increase the normal state resistivity. The critical temperature depends slowly on fluence up to 10^{18} neutrons/cm^2. Most papers report a degradation of the critical temperature T_c together with an increase of the critical current density. Actually, the real evolution is far of being so trivial as usually reported but is decided by the pre-irradiation state of the sample, specifically, on the method used for lithium insertion. Two categories of dependences are discernible, one in which the critical temperature has a peak at low fluences $\Phi \le 10^{17}$ neutrons/cm^2 followed by a continuous decrease at high fluences (Fig. 2) [14-17] and another one in which a slight increase is present at high fluences (Fig. 3).

The low fluence T_c-peak results from the generation-recombination balance of defects produced during irradiation. Assuming the same energy dependent rates of defect production per unit volume, F (E), but different relaxation times, τ_{ch}, $\tau_{p,}$ for chain and, respectively, plane defects one obtains the following time dependence of the defect (vacancy) concentration [19]:

$$n_v(t) = F\tau_{ch} + \left(n_{ch}^0 - F\tau_{ch}\right)\exp\left(-\frac{t}{\tau_{ch}}\right) + F\tau_p\left[1-\exp\left(-\frac{t}{\tau_p}\right)\right] \quad (1)$$

where n_{ch}^0 is the concentration of defects before irradiation and τ's some characteristic times. The rate of the defect generation is dependent on neutron flux, ϕ_0, oxygen concentration, n_O, and the effective cross section, $\sigma_d(E)$ is given by $F = n_O\sigma_d\phi_0$. The relaxation times originate both in thermal diffusion and in radiation stimulated relaxation. The concentration of defects, (1), exhibits a minimum if $n_{ch}^0 > 2F\tau_{ch}$.

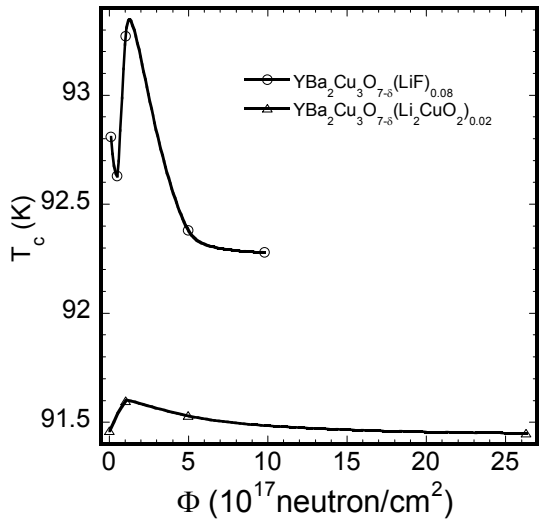

Fig. 2. Critical temperature T_c vs neutron fluence for two samples displaying low fluence peak effect.

The change in the chain oxygen under irradiation shifts the chemical potential closer or farther from relative to the Van Hove singularity. In this way it increases,

respectively, decreases the density of states which is directly related to the critical temperature [18, 19].

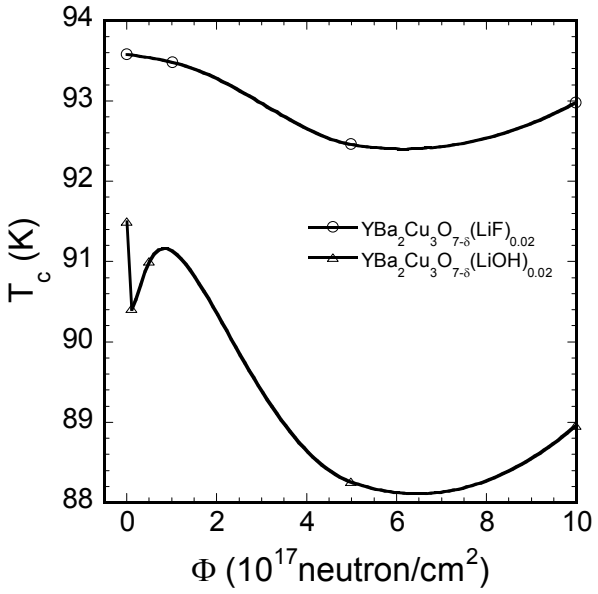

Fig. 3. Critical temperature T_c vs neutron fluence for two samples displaying self organization at high fluence.

In the second case, the increase of the critical temperature at high fluences is the result of a self cleaning process due to the self organization of the defects around some sinks, most likely grain boundary, leaving behind a clean crystal [20]. An example for the evolution of the resistance is presented in Fig. 4 for the samples doped with 2% at. LiCl. The increase of the disorder reaches a maximum at 1×10^{17} neutrons/cm^2 where the disorder goes up to the opening o a pseudogap. The pseudogap opening, which is conspicuous for $\Phi = 1\times10^{17}$ neutrons/cm^2, means that the charge carrier starts to be localized because of the disorder. At higher fluences, the resistance recovers its linear *T*-dependence typical for optimally doped Y-123.

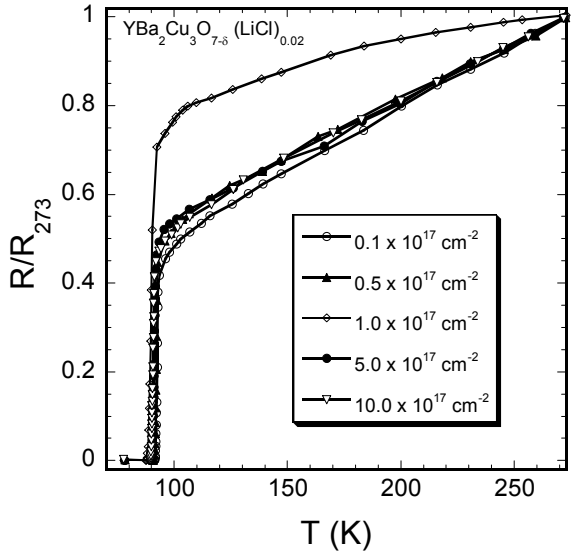

Fig. 4 Dependence of sample normalized resistance vs fluence for a sample of $YBa_2Cu_3O_{7-x}(LiCl)_{0.02}$

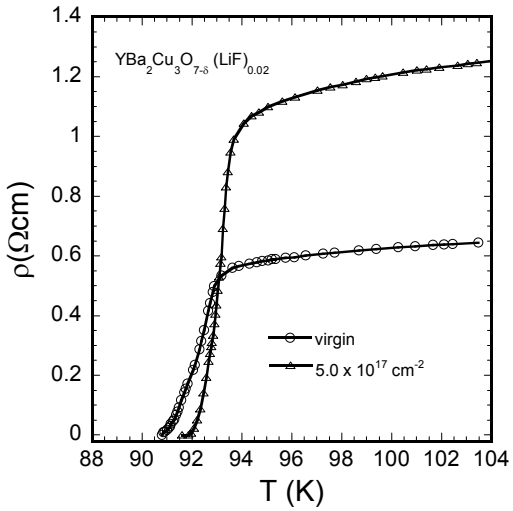

a

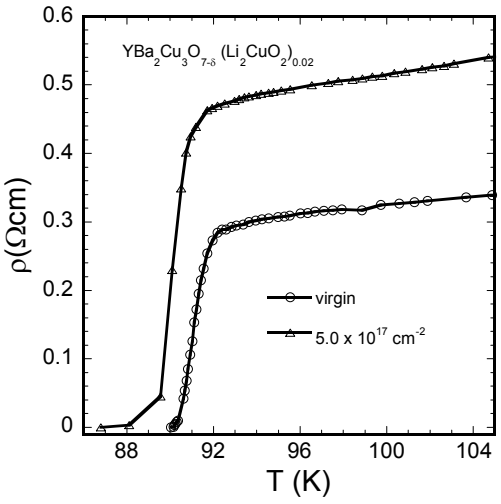

b

Fig. 5 Dependence of the resistivity before and after irradiation for two samples displaying two different behavior: (a) $YBa_2Cu_3O_{7-x}(Li_2CuO_2)_{0.02}$; (b) $YBa_2Cu_3O_{7-x}(LiF)_{0.02}$.

Resistivity evolution at high fluence for the two type of behaviour is presented in Fig. 5 a and b. In both cases the resistivity in normal state increases with Φ, but the transition is shifted to lower temperatures in the case of the samples belonging to the first class of superconducting. The second class of materials behaves differently, with a shift towards higher temperatures after irradiation accompanied, however, with an increase of the normal state resistivity. This fact does not contradict the assumption about irradiative cleaning, because the defects do not disappear, they only self organize themselves and accumulate at grain borders. In this way they also reduce the grain interconnectivity.

The main conclusion is that despite the different mechanisms controlling the transport, the effect of neutron irradiation is weak unless fluences much higher than 10^{18} neutrons/cm^2 are used.

5. Response to an external magnetic field

5.1. Magnetization

The most spectacular effect of irradiation is visible in the magnetic hysteresis loops. The degree of irreversibility of these loops is a measure of the strength of the pinning. Indeed, well pinned vortices face successfully to Lorentz forces and their penetration/exit in/off the sample requires large fields. The simplest estimation of the critical current is given by the well known Bean relationship connecting the critical current density on the irreversible magnetization M_{irr} [21].

$$J_c = a\frac{M_{irr}}{R} \tag{2}$$

where $M_{irr} = \left(M^+ - M^-\right)/2$ with $M^{\pm}$ the ascending (descending) branch of the magnetization loop, a is a constant of order unity depending on sample geometry, and R is the sample or grain mean radius. In the case of the ceramic samples, the magnetization measured for field higher than the full penetration field corresponds to intragrain properties. Below we show several examples showing the evolution of the magnetization after neutron irradiation measured at 77 K. The graphs are representative for the two kind of effects presented above. The samples with a higher density of pre-irradiation defects have a better pinning at high fluences raising with one order of magnitude the critical current density at the highest fluence (Fig. 6a). The samples with a low density of defects before irradiation show a less spectacular increase of J_c, of only three times at the highest fluence.

A general explanation for the increase of the irreversibility, hence, of the critical current resulted from the morphological characteristics. Previously, we have shown that irradiation at fluences of order 5×10^{17} neutrons/cm^2 or higher leads to the proliferation of dislocation loops as well as the precipitation of nanometric $(Cu,Li)_2O$ of size 40-100 Å. A similar effect was found in the case of Y_2O_3 or Ag precipitates of the same size in Y-123. For the pinning on these particles, Matsushita [11] proposed the following relationship:

$$J_c = \left(\frac{N_p}{4\pi a_0^3}\right)^{1/2} \frac{\beta B_c^2 w^2}{2\mu_0 B} \tag{3}$$

with N_p the density of nanoparticles, B_c the critical thermodynamic field, w the particle size, a_0 the intervortex spacing, and $\beta \approx 2$. Fig. 9 shows the fit of the critical current density as extracted with Bean's relationship with Matsushita's dependence (Eq. 3) for a ceramic sample of Y-123 doped with 8% mol LiF. The fit is good for N_p = 6,55x10^{15} cm^{-3} corresponding to an average interparticle spacing of 530 Å given by TEM investigations.

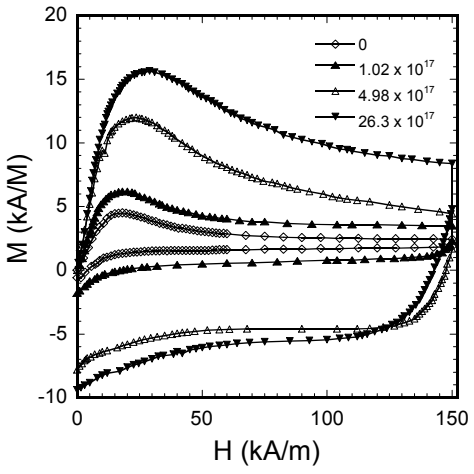

a

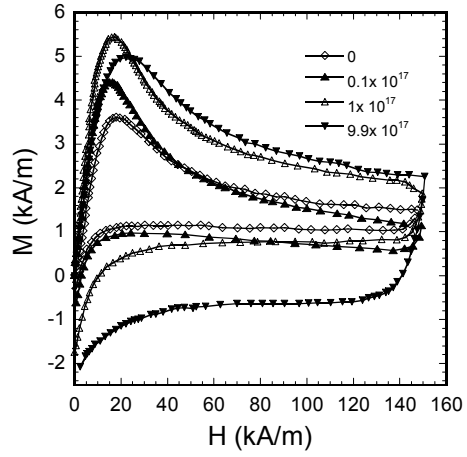

b

Fig. 6. Magnetization loops measured at 77 K for neutron irradiated Li-doped Y-123: (a) via 2% mol Li_2CuO_2; (b) via 2% mol LiF.

The dependence of the critical current density on fluence can be discussed in terms of Van Hove singularity in a manner similar to the critical temperature. This model, together with a δT_c-pinning yields [19]:

$$J_c(\Phi) = j_0^*(T)\left\{1 + \beta_1 \exp\left(-\alpha_1\Phi\right) + \beta_2 \exp\left(-\alpha_2\Phi\right)\right\}^{2/3}$$

Where, α_i and β_i are material dependent constants. Such dependence is reasonably confirmed at low fluences [10].

5.2. Magnetic susceptibility

The measurements of susceptibility on a sample doped with 2 mol % LiF show an improvement of the superconducting properties within grains at fluences of order 10^{18} cm^{-2} in contrast with the depression of these properties after irradiation at fluences of order 10^{17} cm^{-2} (Fig. 7). The fluence dependence of χ_1'' is in agreement with the data of resistivity and magnetization. It advocates

for an improvement relative to the damaged sample irradiated at 0.98×10^{17} cm^{-2}.

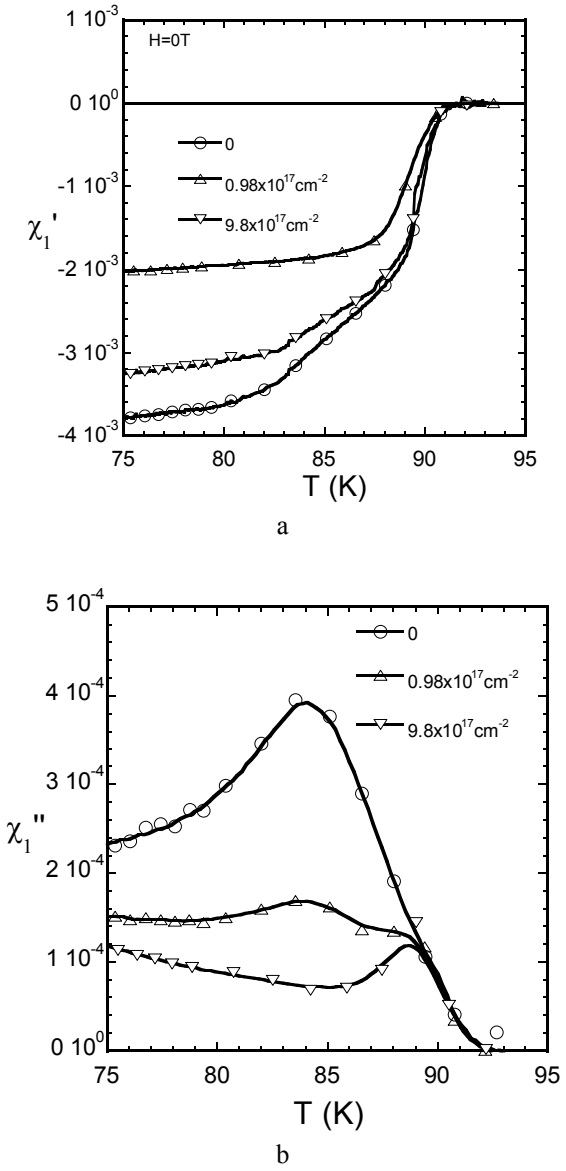

Fig. 7. Ac susceptibility of a $YBa_2Cu_3O_{7-x}(LiF)_{0.02}$ ceramic sample. Fundamental harmonic.

The changes of the third harmonics suggest improvements even relative to the unirradiated sample. The intergranular contribution displays a different dependence on fluence (Fig. 8).

The contrasting behaviour of the two contribution suggests that the almost uniform degradation of the samples irradiated up 0.98×10^{17} neutrons/cm^2, which are evidenced in susceptibility experiments, crosses over into a nonuniform one at 9.98×10^{17} neutrons/cm^2. The latter distribution can be depicted as an accumulation of the defects in the intergranular space causing a rapid degradation of the Josephson connections, hence, shifting the intragranular peak toward very low temperatures, and a "cleaning" of the intragranular area, hence, leaving large defectless areas within grains.

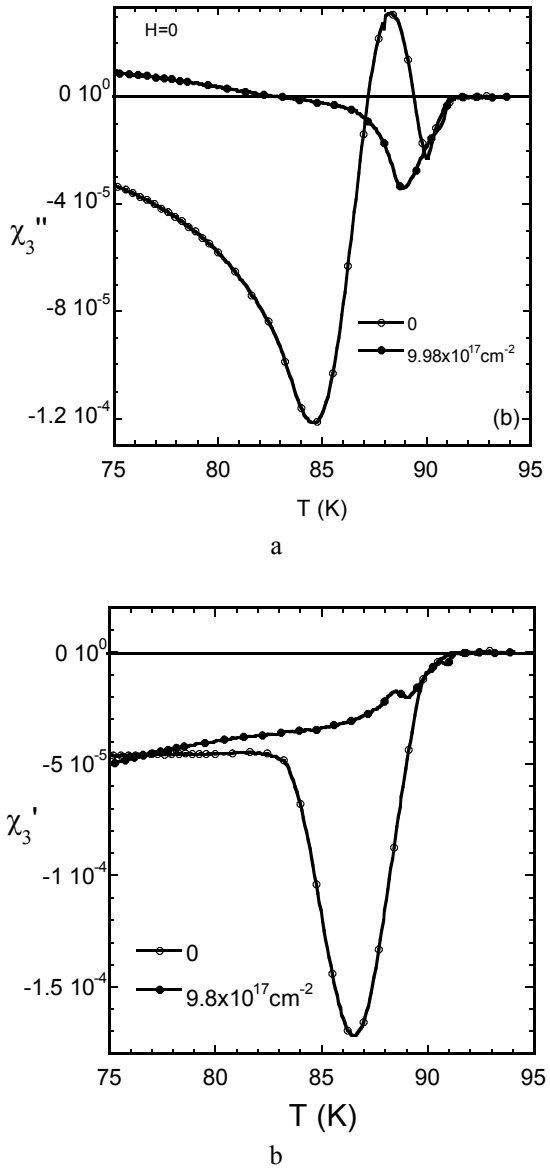

Fig. 8. Ac susceptibility of a $YBa_2Cu_3O_{7-x}(LiF)_{0.02}$ ceramic. Third harmonic.

Such a transition of the defect distribution was predicted by the theory of diffusional reactions applied to irradiation damages. The nonlinear equation describing the complex process of generation, diffusion, and annihilation of the defects possesses a bifurcation point where the homogeneous distribution could become unstable leading to a self-organization of the defect distribution. The self-organization of defects, including pattern formation, occurs when, besides the mobile defects, i.e., vacancies and interstitials, less mobile clusters of vacancies are also

produced due to the higher value of the diffusion constant of interstitials relative to vacations.

It is expected that the grain border should be the sink with the highest strength and bias factor. The point defects, which are absorbed by the border sinks, contribute to the increase of the effective thickness of the intergrain Josephson junction, hence, to the decrease of the sample connectedness. This is a consequence of the exponential decrease of the intragranular lower critical field when the barrier widens.

The diffusion of defects towards all strongly biased sinks leaves back large, defectless areas displaying a local improved superconductivity. It was shown by numerical simulation that a key role in the development of the nonuniform distribution of defects is provided by the material anisotropy.

In conclusion, neutron irradiation is a very efficient way to create a strong pinning. However, the strength of pinning depends on the amount of lithium as well as the vector carrying Li in the sample. Two mechanisms have been found to control the defect evolution. One consists in the dominance of defect recombination at fluences lower than 10^{17} neutrons/cm^2, which is effective for high concentration of pre-irradiative defects. The second is the development of self-organization of the irradiation generated defects at fluences higher than 5×10^{17} neutrons/cm^2.

Acknowledgments

The researches were supported in part by the European Community under the TARI contract HPRI-CT-1999-00088 and by Romanian NARS under the Projects MATNANTECH 260/2004 and CEX 73/2005 at NIMP. We are also indebt to Prof. Florin Vasiliu, Dr. Daniele di Gioacchino, and Dr. Paolo Tripodi for the useful discussions.

References

[1] G. Blatter, M. V. Feigel'man, V. B. Geshkenbein, A. I. Larkin, V. M. Vinokur, Rev. Mod. Phys. **66**, 1125 (1995).
[2] L. Civale, A. D. Marwick, T. K. Worthington, M. A. Kirk, J. R. Thompson, L. Krusin-Elbaum, Y. Sun, J. R. Clem, F. Holtzberg, Phys. Rev. Lett. **67**, 648 (1991).
[3] M. Konczykowski, L. I. Burlachkov, Y. Yeshurun, F. Holtzberg, Phys. Rev. **B 43**, 13707 (1991).
[4] M. Ausloos, C. Laurent, H.W. Vandershueren, A. Rulmant, P. Tast, Solid State Commun. **68**, 539 (1988).
[5] N. A. Fleischer, I. Lyubomirsky, Y. Scolnik, J. Manassen, Solid State Ion Diffusion React. **59**, (1993).
[6] V. Sandu, J. Jaklovszky, E. Cimpoiasu, M. C. Bunescu, J. Supercond. **10,** 231 (1997).
[7] V. Sandu, J. Jaklovszky, E. Cimpoiasu, M. C. Bunescu, Rom. J. Phys. **42**, 217 (1997).
[8] T. Shitamachi et al., Physica C392-396, 254 (2003).
[9] F. Vasiliu, V. Sandu, P. Nita, S. Popa, E. Cimpoiasu, M. C. Bunescu, Physica C **303**, 209 (1998).
[10] G. Van Tendeloo and S.Amelinckx, J. of Electronmicroscopy Technique **8**, 285 (1988).
[11] T. Matsushita, Proc. ISTEC Workshop on Superconductivity, Feb. 1989, Oiso, Japan.
[12] F. J. Gotor, J. Ayache, N. Pellerin, P. Odier**,** J. Mater. Res. **12**, 2 (1997).
[13] M. A. Kirk, M. C.Frischherz, J. Z. Liu, L. R. Greenwood, H.W.Weber, Phil. Mag. Lett., **62**, 41 (1990).
[14] A. Okada, T. Kawakubo, Rad. Effects and Defects in Solids **108,** 137 (1989).
[15] R. F. Konopleva, B. L. Oksengendler, A. K. Pustovoit, B. Borisov, V. A. Chekanov, M. V. Chudakov, Sverkh. Fiz. Him. Tekh. **3,** 568 (1993)
[16] V. Sandu, G. Aldica, S. Popa, E. Cimpoiasu, C. Garlea, I. Garlea, J. Supercond. **8,** 337 (1995).
[17] S. K. Tolpygo, J. Y. Lin, M. Gurvitch, S. Y. Hou, J. M. Phillips, Phys. Rev. **B 53,** 12462 (1996).
[18] C. C. Tsuei, D. M. Newns, C. C. Chi, P. C. Pattnaik, Phys. Rev. Lett., **65**. 2724, (1990).
[19] V. Sandu, S. Popa, J. Jaklovszky, E. Cimpoiasu, J. Supercond. **11**, 251 (1998).
[20] D. Walgraef, N. M. Ghoniem, Phys. Rev. B **39**, 8867 (1989); **52**, 3951 (1995).
[21] C. P. Bean, Phys. Rev. Lett., **8**, 250(1960).

Corresponding author:viorelsandu51@yahoo.com